

Using a Compound Gain Field to Compute a Reach Plan

Steve W.C. Chang,^{1,*} Charalampos Papadimitriou,¹ and Lawrence H. Snyder¹

¹Department of Anatomy and Neurobiology, Washington University in St. Louis School of Medicine, St. Louis, MO 63110, USA

*Correspondence: steve@eye-hand.wustl.edu

DOI 10.1016/j.neuron.2009.11.005

SUMMARY

A gain field, the scaling of a tuned neuronal response by a postural signal, may help support neuronal computation. Here, we characterize eye and hand position gain fields in the parietal reach region (PRR). Eye and hand gain fields in individual PRR neurons are similar in magnitude but opposite in sign to one another. This systematic arrangement produces a compound gain field that is proportional to the distance between gaze location and initial hand position. As a result, the visual response to a target for an upcoming reach is scaled by the initial gaze-to-hand distance. Such a scaling is similar to what would be predicted in a neural network that mediates between eye- and hand-centered representations of target location. This systematic arrangement supports a role of PRR in visually guided reaching and provides strong evidence that gain fields are used for neural computations.

INTRODUCTION

For over 20 years, gain fields have been proposed to comprise a mechanism for neural computation. Modulations of visually evoked responses by eye position were first reported in area 7a and the lateral intraparietal area (LIP) (Andersen and Mountcastle, 1983; Andersen et al., 1990) and were subsequently found in many other cortical and subcortical structures, including V1 (Weyand and Malpeli, 1993), V3A (Galletti and Battaglini, 1989), the dorsal premotor cortex (Boussaoud et al., 1998), parieto-occipital area or V6A (Galletti et al., 1995; Nakamura et al., 1999), superior colliculus (Van Opstal et al., 1995; Groh and Sparks, 1996), and lateral geniculate nucleus (Lal and Friedlander, 1990). Gain fields have been postulated for head position in LIP (Brotchie et al., 1995), attention in V4 (Connor et al., 1996; but see Boynton, 2009), viewing distance in V4 (Dobbins et al., 1998), and eye and head velocity in the dorsal medial superior temporal area (Bradley et al., 1996). A topographical arrangement of gain fields has been suggested in 7a and the dorsal parietal area (Siegel et al., 2003). Gain field modulations may underlie more complex computations such as translation-invariance in inferior temporal cortex (Salinas and Thier, 2000; Salinas and Sejnowski, 2001). In summary, gain fields appear in many parts of the brain, in both dorsal and ventral streams and have been

suggested to be a universal mechanism for neural computations (Salinas and Sejnowski, 2001).

Zipser and Andersen (1988) realized that eye position gain fields might be used to transform the reference frame of eye-centered visual responses into head-centered responses, and built a neural network as an existence proof of this idea. They used back-propagation to train a three layer network with tuned visual inputs (similar to those of V1 and other early visual areas) and a linear eye position input (similar to those found in brainstem eye position neurons and, more recently, in primary somatosensory cortex, Wang et al., 2007) to produce head-centered outputs. The nodes within the middle “hidden” layer have tuned visual responses that are gain modulated by eye position, similar to LIP and 7a neurons. The findings generalize to other training algorithms, architectures and reference frame transformations (Mazzoni et al., 1991; Burnod et al., 1992; Pouget and Sejnowski, 1994; Salinas and Abbott, 1995; Salinas and Abbott, 1996; Xing and Andersen, 2000; White and Snyder, 2004; Smith and Crawford, 2005; Brozovic et al., 2007; Blohm et al., 2009). Based on these data, the hypothesis that gain fields help mediate spatial computations for action is now generally accepted.

In the current study, we present novel findings regarding gain fields in the parietal reach region (PRR). PRR neurons in the posterior portion of the intral parietal sulcus (IPS) are more active when planning a reach than a saccade and have been proposed to play a role in planning visually guided arm movements (Snyder et al., 1997; Andersen et al., 1998; Calton et al., 2002). PRR straddles the boundary between the medial intraparietal area (MIP) and V6A (Snyder et al., 1997; Calton et al., 2002; Chang et al., 2008). Tuned PRR neurons encode the target for an upcoming reach to a visual or auditory target, or discharge during reaching movements (Caminiti et al., 1996; Galletti et al., 1997; Batista et al., 1999; Cohen and Andersen, 2000; Battaglia-Mayer et al., 2001; Fattori et al., 2001; Buneo et al., 2002; Marzocchi et al., 2008). Under certain circumstances, PRR activity predicts reach reaction time and endpoint (Snyder et al., 2006; Chang et al., 2008; Quian Quiroga et al., 2006). Eye and hand position effects in PRR have been reported (Andersen et al., 1998; Batista, 1999; Cohen and Andersen, 2000; Buneo et al., 2002; Marzocchi et al., 2008) but not quantified.

We now report that eye and hand position gain fields in PRR are systematically configured to encode the distance between the point of gaze fixation and the position of the hand. We refer to this as “eye-hand distance,” and the gain mechanism based on this distance, “eye-hand distance gain field,” or simply “distance gain field.” We define a hand-centered representation

of target position as the location of the target in a coordinate system whose origin coincides with the location of the hand, or, equivalently, a vector extending from the location of the hand to the target. In a two-dimensional system, eye-hand distance is required to transform eye-centered visual target information into hand-centered visual target information (Bullock and Grossberg, 1988; Buneo et al., 2002; Shadmehr and Wise, 2005; Blohm and Crawford, 2007). The eye-to hand-centered transformation is crucial for reconciling information from different modalities related to arm movements and for generating a motor command to a visible target. The identification of an explicit eye-hand distance gain field supports a role of PRR in these processes and adds to the evidence that gain fields are indeed used by the brain for certain spatial computations.

RESULTS

We recorded neuronal activity in PRR and identified 259 well-isolated, stable cells that showed spatial tuning (see [Experimental Procedures](#)). For each neuron, we first mapped its preferred direction and then ran a delayed visually guided reaching task designed to measure eye and hand position gain fields. The task began with the animal touching an initial hand position target and looking at an initial eye position target. There were five different configurations of initial eye and hand positions: eyes and hand aligned at center, hand at center and eyes to the right or left, and eyes at center and hand to the right or left (Figure 1A). A peripheral reach target then appeared at one of eight locations, five of which were arrayed about the preferred direction (Figure 1A). After a variable delay the initial target shrank in size, cueing a reach (but no eye movement) to the peripheral target (Figure 1B).

Cells were recorded from two animals (102 and 157 from monkey G and S, respectively). The reconstructed recording locations for neurons straddle the border between V6A and MIP (Lewis and Van Essen, 2000a, 2000b; C. Galletti, personal communication), with a few cells on the lateral bank (Figure 1C). These locations match those reported in previous studies of PRR (Snyder et al., 1997; Calton et al., 2002; Chang et al., 2008).

Animals performed the task well, successfully completing 89% and 96% of the initiated trials (monkeys G and S, respectively) with a median reach response latency of 238 ± 76 ms and 246 ± 55 ms (\pm SD). Table 1 shows median eye and hand distance from the initial eye targets, initial hand targets, and final reach targets.

Single Neuron: Eye and Hand Gain Fields

Responses to the five targets near the preferred direction were tuned, and for most neurons the tuning was a function of the initial eye and hand configuration. For the example neuron in Figure 2A, when the eye and hand were initially aligned at the central position (*Aligned*), the delay period activity was strongest for the center target (T3). When the starting eye position was displaced to the left (*Eyes Left*) or right (*Eyes Right*), the greatest delay activity was evoked by a target shifted one position to the left (T2) or to the right (between T3 and T4), respectively. In contrast, when the starting hand positions were displaced to the left or right, the peak did not shift, but instead remained at

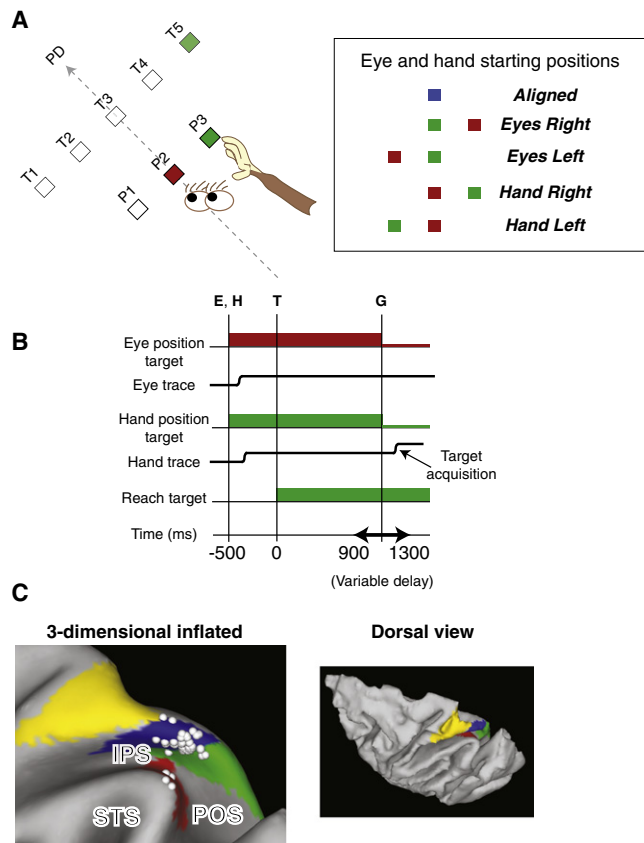


Figure 1. Behavioral Task and Anatomical Locations of Recorded PRR Neurons

(A) Animals reached to one of eight illuminated targets (only the five targets in or near the preferred direction are shown, T1–T5; see text) from one of five initial eye and hand target positions (box). In one condition, animals looked at and touched a central target (P2; *Aligned* condition). In the other four conditions, animals touched the center target and fixated P1 or P3 (*Eyes Left* or *Eyes Right*), or else fixated the center target and touched P1 or P3 (*Hand Left* or *Hand Right*). For each recorded neuron the preferred direction (PD) for reaching was first estimated and then targets and initial eye and hand target positions were arranged relative to the PD, as shown. All conditions and targets were fully interleaved.

(B) The temporal sequence of the task. Time zero corresponds to the time of reach target onset. E: eye position target onset, H: hand position target onset, T: reach target onset, and G: go signal.

(C) The anatomical locations of the neurons from one animal (G) are shown on an inflated cortical map using Caret software (<http://brainmap.wustl.edu/caret/>). Cortical areas are color-coded according to Lewis and Van Essen (2000a, 2000b). Green: PO/V6A (Galletti et al., 1999); blue: MIP; yellow: dorsal area 5 (5D); red: the lateral occipitoparietal area (LOP).

the central target (*Hand Left* and *Hand Right*). Tuning shifts with changes in initial eye position but not with changes in initial hand position are consistent with an eye-centered representation of target location (Batista et al., 1999).

Activity did not only shift with changes in initial configuration; it also showed systematic increases or decreases in amplitude (Figure 2A). Peak activity was much greater when initial fixation was to the left compared to the right (middle row, *Eyes Left* versus *Eyes Right*; 17.50 ± 3.09 sp/s versus 8.75 ± 2.06 sp/s

Table 1. Median Absolute Distance of Eye and Hand from the Initial Hand, Initial Eye and Final Reach Targets

Animal	Absolute Initial Hand Position Error (Deg; Median \pm SD)		Absolute Eye Position Error		Absolute Final Hand Position Error	
	Horizontal	Vertical	H	V	H	V
G	2.35 \pm 2.09	1.80 \pm 1.60	0.90 \pm 0.88	1.19 \pm 1.05	2.40 \pm 2.31	2.11 \pm 2.08
S	1.85 \pm 1.79	1.34 \pm 1.10	0.60 \pm 0.55	0.74 \pm 0.65	2.05 \pm 1.92	1.30 \pm 1.26

[mean \pm SEM]; Wilcoxon rank sum test, $p = 0.08$), and activity was much greater in *Hand Right* than *Hand Left* (bottom row; 13.04 \pm 3.21 sp/s versus 23.21 \pm 2.51 sp/s; $p < 0.05$). The eye and hand gain effects were opposite in direction but similar in magnitude; there was no significant difference between the peak activity for *Eyes Left* versus *Hand Right* ($p = 0.13$), nor between *Eyes Right* versus *Hand Left* ($p = 0.43$).

In order to more precisely measure gain field effects, the data were fit to a seven parameter model that allowed Gaussian tuning in a frame of reference centered on the fixation point (eye-centered), on the starting hand position (hand-centered), or on any point along a line connecting those two points (Equa-

tion 1). The model included separate eye and hand position gain field terms. The fit for the example neuron (Figure 2B) accounted for 89% of the variance across conditions ($r^2 = 0.89$). This fit included an eye gain field of -0.76 sp/s per deg and a hand gain field of 0.85 sp/s per deg. The unsigned amplitudes (0.76 and 0.85 sp/s/deg) were statistically indistinguishable (two-tailed t test, $p = 0.79$). To test the significance of the two gain fields, we compared the seven parameter “full” model with two “reduced” six parameter models, each the same as the original model but one lacking an eye gain field and the other lacking a hand gain field (Experimental Procedures). The full model accounted for significantly more variance than either of

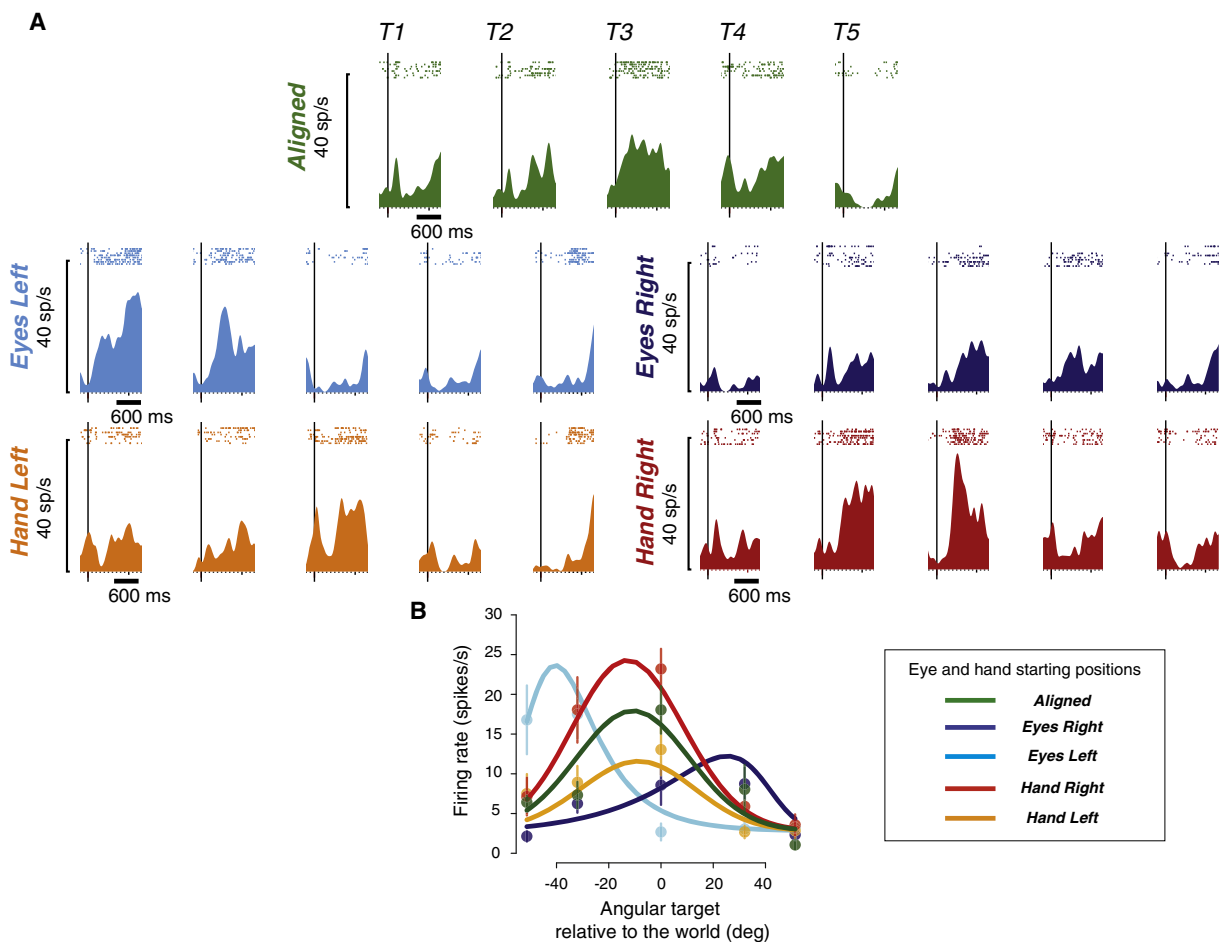


Figure 2. Eye and Hand Position Gain Fields in a Single PRR Neuron Are Similar in Strength but Opposite in Sign

(A) Peristimulus time histograms and rasters of an example neuron are shown for five initial eye and hand positions (see the box in Figure 1A for the color code) for the five target locations (T1–T5). Delay activity is shown, with data aligned to the time of target presentation (vertical line).

(B) Mean firing rates, SEM (circles plus bars), and fitted tuning curves (Equation 1) from the delay interval are shown as a function of angular target location relative to the world.

the two reduced models, demonstrating that both the eye and hand position gain fields were highly significant (two-tailed sequential F test, $F = 12.21$ and 16.25 , respectively, $p < 0.00001$ for both comparisons).

Population: Model Fit

A total of 259 neurons were recorded from PRR in two monkeys. Model fits were judged based on how well the model accounted for firing rate, based initially on several different tests. For the delay interval, a Chi-square test of the goodness of fit accepted 161 (62%) of the neurons ($p > 0.05$). For these cells, the median Gaussian amplitude was 9.87 sp/s, and the median variance explained was 67%. Of the 259 cells, 61% (158) had an r^2 value of at least 50%. The variance explained (r^2) criterion (>50%) accepted some cells that showed minimal modulation across conditions (target position, initial eye and hand position), and for these neurons the fit sometimes appeared spurious (see Figure S1 available online for an example). We therefore combined the amplitude of Gaussian tuning described by the model and the variance explained [r^2] by multiplying the two factors together to produce a single measure of “spike-variance explained,” with units of spikes per second. Roughly, spike-variance explained quantifies the variance in our responses (in sp/s) that were driven by our manipulations of target position. For example, a cell with r^2 of 60% that showed 40 sp/s modulation to target positions would have 24 sp/s spike-variance explained. A cell with an r^2 of 15% and 40 sp/s of modulation, or a cell with an r^2 of 60% and 10 sp/s of modulation, would each have a spike-variance explained of only 6 sp/s.

Using spike-variance explained, 176 of 259 cells (67%) met or exceeded a criterion of 2 sp/s, and 103 cells (40%) met or exceeded a criterion of 5 sp/s (61 and 42 cells for monkey G and S, respectively; monkey G cells are plotted in Figure 1C). Each criterion (Chi-square test, variance explained greater than 50%, spike-variance explained greater or equal to 2 or 5 sp/s) resulted in a similar conclusion with regard to eye and hand gain fields (see below). Note that none of these criteria required that the gain field terms of the model be different from zero.

Population: Eye and Hand Gain Fields Are Negatively Correlated

Across neurons with at least 5 sp/s of spike-variance explained, the median absolute eye position gain field was 3.44% of peak activity per deg and the median absolute hand position gain field was 2.08%/deg. Within each cell, eye and hand position gain fields were negatively correlated (Spearman's rank correlation, $r = -0.61$, $p < 0.00001$; type II regression slope = -0.74 ; Figure 3A and Figure S2). This relationship was clearly present when the data from each monkey is considered separately (monkey G: $r = -0.68$, $p < 0.00001$, slope = -0.78 ; monkey S: $r = -0.47$, $p < 0.005$, slope = -0.67). Only four cells showed a significant difference (two-tailed t test, $p < 0.05$) between the fitted eye position gain field parameter and the negative of the fitted hand position gain field parameter. The number of cells showing a difference is not significantly different from that expected by chance, even if all cells are in fact correlated, given the criterion p value of 0.05 (proportion test, $p = 0.77$). The data points are evenly distributed about the negative unity line

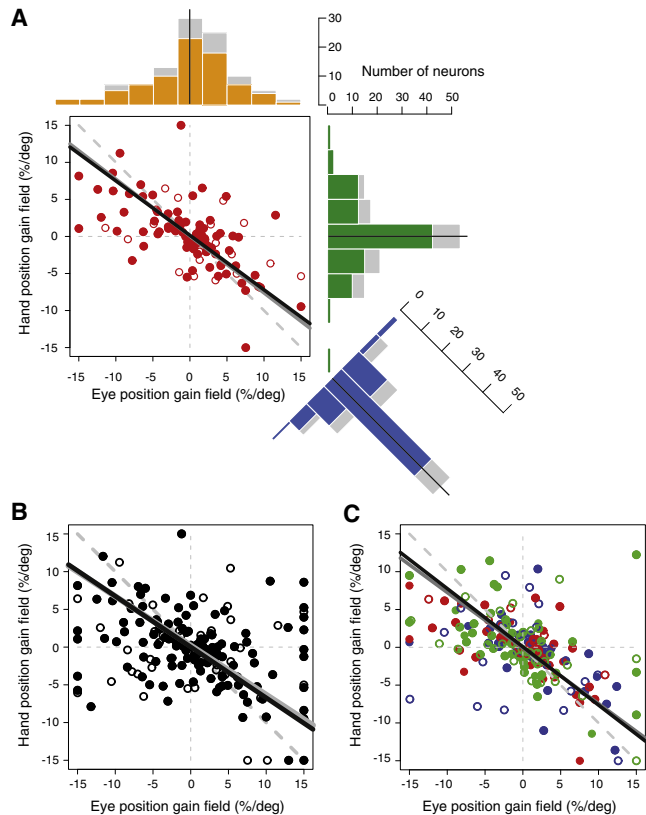


Figure 3. PRR Neurons Encode the Distance between the Initial Eye and the Hand Positions Using Negatively Coupled Eye and Hand Position Gain Fields

(A) Each data point represents gain field amplitudes (%/deg) during the delay interval for one neuron ($n = 103$). Filled points ($n = 79$) indicate cells with at least one significant gain field (sequential F -test, $p < 0.05$). Two marginal histograms show the distribution of eye (yellow-orange) and hand (green) position gain fields. The third histogram shows the distribution of the orthogonal distance from the negative unity line (dashed line). Grey shading indicates cells without significant gain field effects. The solid black and gray lines represent the type II regressions for all cells and for the significant cells, respectively.

(B) The negative correlation between eye and hand position gain fields (delay interval) is present even when the acceptance criterion was relaxed to 2 sp/s of spike-variance explained (174 cells). Same format as (A).

(C) Gain field relationship across different task intervals. Each data point (a cell) was chosen from one of the three task intervals (visual, delay, perimovement) which showed the highest spike-variance explained ($n = 155$). Blue: visual; red: delay; green: perimovement. Filled points ($n = 134$) indicate cells with at least one significant gain field. Same format as (A).

($y = -x$), consistent with the two gain fields being similar in magnitude but opposite in sign (blue oblique marginal histogram, Figure 3A). If we eliminate those cells for which neither gain field is significant (24 cells, based on a sequential F -tests), there is an even stronger negative relationship between the eye and hand gain fields (Spearman's rank correlation, $r = -0.66$, $p < 0.00001$, reg. slope = -0.77).

If the acceptance criterion is relaxed to 2 sp/s of spike-variance explained in order to include 67% of our recorded cells, the significant negative coupling between eye and hand gain fields remains (174 cells, $r = -0.29$, $p < 0.0001$; reg. slope = -0.67 ;

Figure 3B). Even when all the cells for which our model converged are considered (254 cells, 98%), a slope of -0.81 and significant negative correlation ($r = -0.14$, $p < 0.05$) are obtained (data not shown).

The negative correlation between the two gain fields was not restricted to the delay period. From each cell, we selected the interval—visual, delay, or perimovement—with the largest variance explained of the three. Cells were included if the model explained at least 5 sp/s of spike-variance (155 cells) in that interval. The strong negative relationship between eye and hand gain fields persisted ($r = -0.56$, $p < 0.00001$, reg. slope = -0.77 ; 134 cells with either significant eye or hand gain field: $r = -0.62$, $p < 0.00001$, reg. slope = -0.73 ; Figure 3C). Again, only four cells showed a significant difference between the fitted eye position gain field parameter and the negative of the fitted hand position gain field parameter (not different from chance by proportion test, $p = 0.23$). We also observed the negative correlation between the two gain fields when we looked at each interval alone, without pooling across intervals (visual interval: $r = -0.53$, $p < 0.00001$, reg. slope = -0.91 , $n = 103$; perimovement interval, $r = -0.64$, $p < 0.00001$, reg. slope = -0.80 , $n = 117$).

The distance gain field was established as soon as the animals acquired the initial eye and hand targets. Prior to the appearance of a final reach target but after acquiring the eye and hand initial targets, the two gain fields were already negatively correlated (71 cells with at least 5 sp/s spike-variance explained: $r = -0.63$, $p < 0.00001$, reg. slope = -0.68 ; 143 cells with at least 2 sp/s spike-variance explained: $r = -0.49$, $p < 0.00001$, reg. slope = -0.80 ; all cells: $r = -0.38$, $p < 0.00001$, reg. slope = -0.80 ; Figure S3). The gain fields established before and after the onset of a reach target were strongly correlated. This strong correlation was present for both for eye gain fields ($r = 0.52$, $p < 0.00001$, $n = 104$) and for hand gain fields ($r = 0.38$, $p < 0.0001$, $n = 104$; Figure S4).

The slopes of the regressions in Figure 3 are close to but significantly smaller than -1 (linear regression, all $p < 0.05$). This was also true when the data from each monkey were considered separately, regardless of the criteria used to select neurons. See Supplemental Data for more detail.

Negatively Correlated Gain Fields Are Equivalent to a Gain Field for Eye-Hand Distance

Our “full model” (Equation 1 in Experimental Procedures) posits that eye and hand gain fields add together. In other words, the combination of an eye gain field of 3%/deg and a hand gain field of -3% would produce a total modulation of 0%. More generally, gain fields of similar magnitude but opposite sign that add together would be identical to a single gain field encoding the signed distance between the fixation point and the hand (Equation 2). To test this idea, we fit the data using a six parameter model in which the two separate gain field terms from the full model were replaced with a single gain field term for eye-to-hand distance. Despite having one fewer parameter, the new model has similar spike-variance explained for most neurons (Figure 4A). The median distance gain field in this model is 2.30%/deg. On average, the full model explains only 0.43 sp/s of variance more than the model with a single distance gain field.

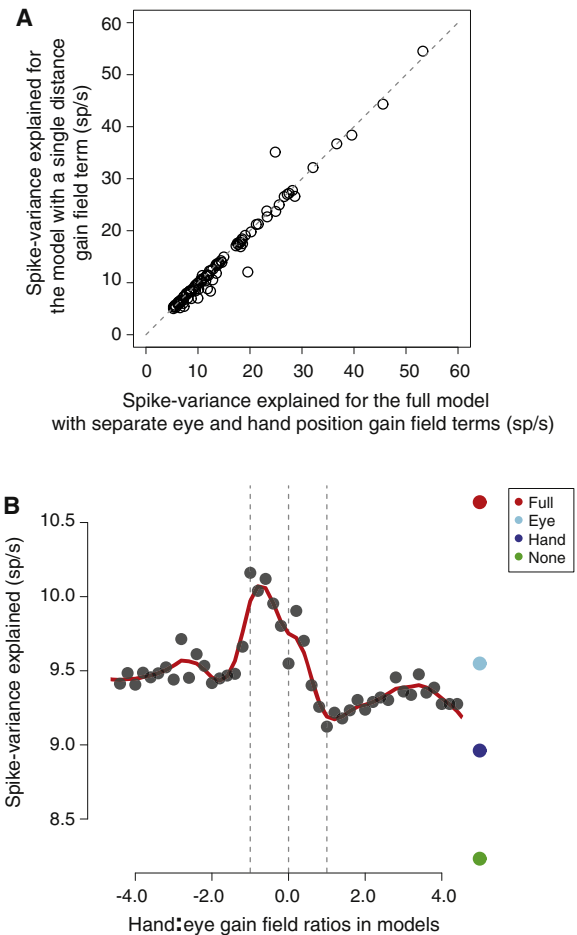


Figure 4. A Single Distance Gain Field Model Does Just as Well to Explain the Data as the Separate Eye and Hand Gain Field Model

(A) Spike-variance explained values obtained by fitting each individual neuron’s data (delay interval) to the full model with separate eye and hand gain field terms (Experimental Procedures, Equation 1), and to the model with a single distance gain field term (Equation 2). Despite having one fewer parameter in the distance gain field model, the two models perform similarly. Variance explained cannot be greater in the reduced compared to full model. But the estimate of the amplitude of tuned modulation is not constrained in this way, so spike-variance explained could be larger in the reduced compared to full model.

(B) Spike variance explained by fitting the delay interval data to models with a range of hand-to-eye gain field term ratios. For each model, the eighthy percentile of spike-variance explained is plotted, together with a spline interpolation (red curve). Isolated colored data points show the spike-variance explained by the full model (red), the reduced model with only an eye position gain field (cyan), the reduced model with only a hand position gain field (blue), and a model with no gain fields (green).

Using the Bayesian information criterion ($k = 25$), the fit was judged to be better in the distance gain field model than in the two gain field model in 66% of the cells.

To test whether a different ratio of eye gain field to hand gain field might provide a better fit to the data, we fit the data to a range of models with a single gain field term but varied the ratio of the hand to eye gain field from $-4.5:1$ to $4.5:1$, with a 0.2 increment. Figure 4B shows the eighthy percentile of spike-variance

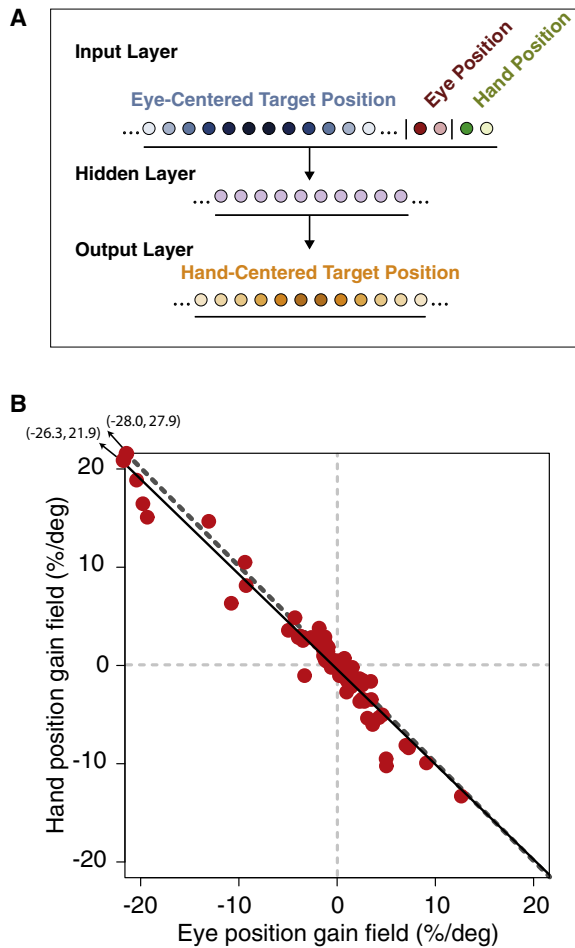


Figure 5. A Neural Network Also Uses a Systematic Arrangement of Eye and Hand Gain Fields

(A) A three-layer network was trained, using feedforward back-propagation algorithm, to convert eye-centered target information (input layer) into hand-centered target information (output layer). The network also received eye position and hand position information as inputs.

(B) Hidden layer nodes from the trained network in (A) had a range of eye and hand position gain field strengths that tended to be similar in magnitude and opposite in sign from one another (type II linear regression slope = -0.97). The dashed line represents the negative unity line.

explained per cell. (We plot the eightieth percentile of spike-variance explained in order to capture the effect of the ratio on the well-fit cells, maximizing the sensitivity of the measure.) The maximum spike-variance explained occurs when the eye gain is equal to -1 times the hand gain, although values slightly less than -1 perform nearly as well.

A Trained Neural Network Produces Eye-Hand Distance Gain Fields

To test for a potential role of eye and hand position gain fields in visually-guided reach transformations, we trained a three-layer network to perform a coordinate transformation analogous to that of the Zipser-Andersen network (Figure 5A). Feed-forward models have been shown to accurately account for realistic

reference frame transformations in two or three dimensions (Zipser and Andersen, 1988; Blohm and Crawford, 2007; Blohm et al., 2009). Tuned visual inputs similar to those of V1 and separate linear eye position inputs (similar to those found in the brainstem eye position neurons) and linear hand position inputs were provided, and the network was trained via back-propagation to produce tuned hand-centered outputs. The hidden layer nodes of these trained networks had tuned eye-centered visual responses that were gain field modulated by both eye and hand position, and these gain field coefficients were negatively correlated with one another, very much as in PRR (Figure 5B). Across nodes, the eye and hand position gain field strengths span a wide range (1.21 ± 5.39 and $1.16 \pm 5.06\%/deg$ [unsigned median \pm SD], respectively; both significantly different from zero: $p < 0.00001$, Wilcoxon signed rank), but in any one node, the eye and hand gain fields were similar in magnitude but opposite in sign to one another (Spearman's rank correlation, $r = -0.95$, $p < 0.00001$). This results in a gain field representation of eye-hand distance.

DISCUSSION

Neurons in PRR selectively encode spatial targets for upcoming reaches using a receptive field code (Snyder et al., 1997; Batista et al., 1999). We now show that visual, memory, and motor responses are modulated in proportion to eye and hand position (gain fields). Within each PRR neuron, eye and hand gain fields are similar in strength but opposite in sign to one another (Figures 2 and 3). Two individual gain fields that are systematically related in this manner and whose effects add linearly are almost indistinguishable from a single gain field for the distance between gaze location and initial hand position (eye-hand distance).

There are at least two roles that a gain field for eye-hand distance might play in PRR. First, the gain field could help implement a transformation from eye- to hand-centered coordinates. Visual information in the early visual areas that project to PRR is referenced to the fovea (eye-centered), and many neurons in PRR are eye-centered (Batista et al., 1999). Motor commands for a reaching movement are necessarily referenced to muscles or joints. Compared to PRR, primary motor and premotor cortex use representations that are closer to "motor coordinates," e.g., a hand-centered frame of reference that takes into account arm geometry (Caminiti et al., 1991; Scott et al., 1997; Herter et al., 2007; but see also Pesaran et al., 2006; Batista et al., 2007). Eye-hand distance gain fields in PRR might help to mediate the first step in this transformation. A second possibility is that PRR neurons may integrate information from different sensory streams into a single representation of target position. We discuss each of these possibilities in turn.

Reference Frame Transformation

Transforming a location from an eye-centered to a hand-centered reference frame in one or two dimensions requires subtracting the eye-hand distance from the eye-centered target location (Bullock and Grossberg, 1988; Shadmehr and Wise, 2005). In three dimensions, movements of the eyes to tertiary (oblique) positions or roll movements of the head will rotate the retina about the line of sight, complicating these transformations

(Crawford and Vilis, 1991; Tweed and Vilis, 1987; Smith and Crawford, 2005; Blohm and Crawford, 2007; Blohm et al., 2009). Even secondary eye positions can lead to non-linear reference frame transformations if the hand vector is orthogonal to the direction of eye deviation (e.g., a horizontal hand movement executed when the eye are positioned upward) (Crawford et al., 2000). In many cases, however, the computation reduces to the vector subtraction of the eye-hand distance vector (e.g., when the eye-hand distance is small, or when the eyes are centered and the head is upright; e.g., see Crawford et al., 2004). Vector subtraction is trivial when both postural information and target location are encoded using a proportional rate code in a Cartesian coordinate frame. Indeed, posterior parietal neurons often encode postural information (eye, hand, or head position) using a rate code (Andersen and Mountcastle, 1983; Brotchie et al., 1995). However, the visual system uses a receptive field code, or place code, to represent target locations (Poggio, 1990). Implementing a vector subtraction using a combination of place-coded and rate-coded signals is not trivial (Mays and Sparks, 1980). A neural network solves this task with gain fields in the hidden layer (see Introduction). We now report that both a neural network model (Figure 5) and individual neurons from PRR (Figures 2 and 3) contain eye and hand position gain fields, and that in both systems these gain fields are similar in strength but opposite in sign. These findings are consistent with PRR transforming visual spatial information from an eye- to a hand-centered frame of reference (Figure 6).

Sensory Integration

A possible alternative role for PRR is that it may integrate information from different sensory systems to produce a single unified representation (Lacquaniti and Caminiti, 1998). In order to perform a reach to a visible target, the brain must reconcile visual and proprioceptive or efference copy information (Sober and Sabes, 2003, 2005; Ren et al., 2006). We have just shown that PRR contains gain fields for eye-hand distance. These representations are rate coded, consistent with a derivation from proprioception or efference copy signals (see discussion below). PRR also contains eye-centered representations of target locations, coded using receptive fields, consistent with a derivation from visual input (Batista et al., 1999). PRR might also receive visually-derived information regarding arm position. Some PRR neurons code target location in hand-centered coordinates using a receptive field code (S.W.C.C. and L.H.S., unpublished data; Batista, 1999; Figure 4E in Buneo et al., 2002). While this representation could reflect the output of a reference frame transformation (see previous section), it could also reflect an independent input, derived directly from visual information (Graziano, 1999; Graziano et al., 2000; Buneo et al., 2002). In this case, the three pieces of information (proprioceptive information about eye-hand distance, visual information about target position relative to the eye, and visual information about target position relative to the arm) would be derived from two independent sources (vision and proprioception). Information from these two sources will contain uncorrelated noise and so should be combined in a statistically optimal fashion to obtain the best possible estimate of target location. Pouget and colleagues have proposed that a reciprocal neural

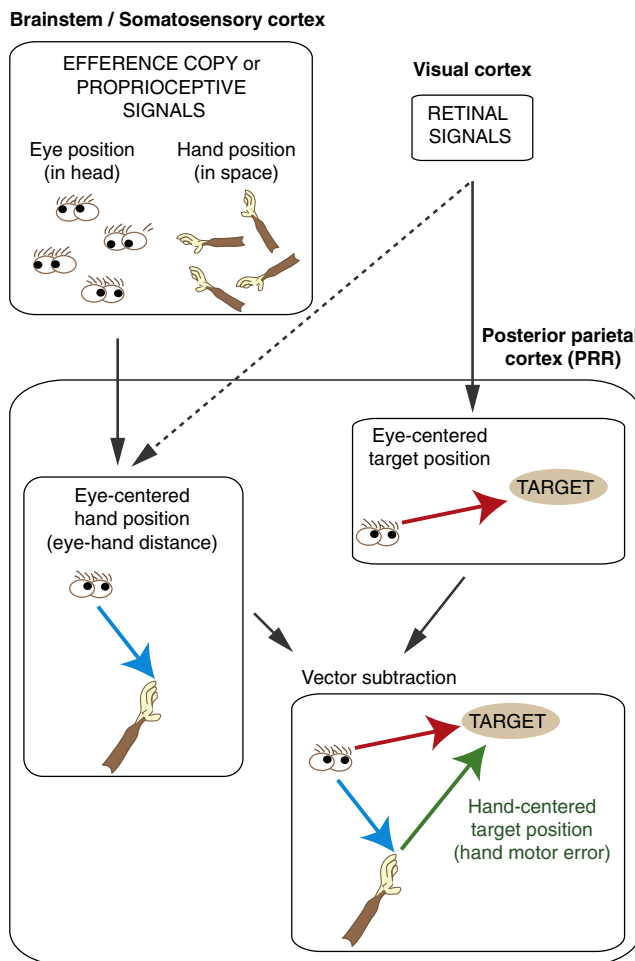


Figure 6. A Schematic of a Proposed Coordinate Transformation Mediated by PRR

PRR receives retinal signals from early visual areas that encode objects in eye-centered coordinates (upper right). PRR also receives eye position and hand position signals, likely from the brain stem and somatosensory cortex (upper left). Within or prior to entering PRR (center), eye and hand position signals could be systematically combined to produce eyes-to-hand distance. This distance could also be directly extracted from the visual scene (dashed arrow), though the fact that the distance is encoded using gain fields rather than receptive fields makes a visual source less likely (but see Sober and Sabes, 2003). Using gain fields, the eye-hand distance could then be subtracted from the eye-centered target position to generate hand-centered target position, which is the desired hand motor error. See text for an alternative proposal in which PRR mediates between eye- and hand-centered information but does not perform an explicit reference frame transformation.

network can be used for this task (Pouget and Sejnowski, 1994; Pouget and Snyder, 2000; Pouget et al., 2002; Avillac et al., 2005). Their proposal suggests that the intermediate layer, like PRR, would show gain fields. Furthermore, PRR is also involved in planning auditory-guided reaches (Cohen and Andersen, 2000). Therefore it is plausible that PRR plays a role in reconciling information from different sensory systems (visual, proprioceptive, auditory) for the ultimate goal of planning reaching movements.

Gain Fields

Eye position gain fields are particularly common in visual pathways (Lal and Friedlander, 1990; Weyand and Malpeli, 1993; Galletti and Battaglini, 1989). Eye position gain field signals are more likely to derive from efference copy than from proprioception (Prevosto et al., 2009). Proprioceptive signals could come from somatosensory area 3a, but these signals are too slow for mediating spatial computations for action (Wang et al., 2007). Furthermore, extraocular muscle proprioception is not necessary for monkeys to perform either double step saccades (Guthrie et al., 1983) or visually guided reaching (Lewis et al., 1998), suggesting that efferent eye position signals are sufficient. Although the idea that gain fields support neuronal computations is well-supported by modeling studies, there is no direct evidence that gain fields are used for computation.

LIP has been proposed to play a role in identifying salient targets to which a saccade might be directed (Snyder et al., 1997; Gottlieb et al., 1998; Kusunoki et al., 2000; Goldberg et al., 2002; Dickinson et al., 2003). Since visual information arrives in an eye-centered frame of reference, and since saccades are performed in an eye-centered frame of reference, is there a need for eye position signals? Parsing a gaze movement into an eye and head component requires information about current eye-in-head position. However, this computation could take place downstream of the parietal cortex, in the colliculus or brainstem (Mays and Sparks, 1980; Robinson et al., 1990; Crawford et al., 1991; Van Opstal et al., 1995; Groh and Sparks, 1996; Pare and Guitton, 1998; Groh et al., 2001). One argument for the use of eye position signals is that accurate execution of large saccades from tertiary eye positions (associated with ocular rotation about the line of sight) and in some cases from secondary eye positions, requires a knowledge of eye position (Crawford and Guitton, 1997; Crawford et al., 2000). Despite this argument, the role of eye position gain fields remains uncertain (Wang et al., 2007; Blohm et al., 2009).

A stronger argument could be made for gain fields subserving computation if the format of a gain field could be shown to be clearly related to the presumed function of an area, where that function was determined independently of the observation of the gain field. Area LIP does not provide such an example, since LIP was first proposed to play a role in reference frame transformations involving eye position precisely because eye position gain fields were observed in its neurons (Zipser and Andersen, 1988). Furthermore, the eye position gain fields in LIP, as in many other cortical areas, do not show a systematic relationship with, for example, receptive field location. While LIP receptive fields are primarily contralateral, gain fields are oriented in all directions (unpublished data; Bremmer et al., 1998). (Similarly, eye gain fields in PMd operate in both contralateral and ipsilateral directions, Boussaoud et al., 1998.) This lack of systematicity is not evidence against the use of gain fields, because theoretical models of coordinate transformations indicate that a population of cells coding a diverse combination of variables, including gain fields, may be particularly desirable (Pouget and Sejnowski, 1994; Pouget and Snyder, 2000; Pouget et al., 2002; Blohm et al., 2009). However, the identification of a systematic relationship between gain fields and a computational goal would

strengthen the claim that gain fields are in fact used for neural computations.

Coding of eye-hand distance using a compound gain field is exactly the form that one would expect if gain fields are to play a critical role in mediating between eye- and hand-centered representations of target locations (Bullock and Grossberg, 1988; Desmurget et al., 1999; Shadmehr and Wise, 2005; Buneo et al., 2002). The fact that this relationship exists is strong evidence that PRR gain fields are constructed for a specific computational purpose. While computational models suggest that a more haphazard arrangement of eye and hand gain fields could be used instead, such a combinatorial representation suffers from the curse of dimensionality: as more variables (e.g., target position, eye position, and hand position) are added to a network using such a non-systematic organization, exponentially more neurons are required for the representation. By requiring eye and hand gain fields to be similar and opposite, many fewer neurons are required to accomplish particular transformations.

There is no reason to believe that compound gain fields are unique to PRR. In fact, some LIP neurons have gain fields for both eye-in-head position and for head-on-body position. These gain fields tend to be matched in scale, and therefore can be thought of as comprising a compound gain field that encodes gaze relative to body (Snyder et al., 1998). Other potential modulatory influences have either not yet been tested or not been tested in a paradigm that will distinguish effects due to gain fields versus effects due to tuning shifts (Mullette-Gillman et al., 2009). An area involved in orienting the head toward visible targets (speculatively, area VIP), or an area involved in orienting the eyes to auditory targets, for example, might contain compound gain fields for the distance between head and eye position. Many other configurations are possible and have yet to be tested.

We sampled five configurations of eye and hand position and assumed that the gain field effects are linear between the two gain fields, that is, additive (Equation 1) rather than, for example, multiplicative (Equation 3). Our conclusion that eye-hand distance is coded by the combined gain fields is dependent on this assumption. However, unless the eye, hand, and target are a substantial distance apart, there is minimal difference between the additive and multiplicative models (see Equations 3 and 4 and associated text in [Experimental Procedures](#) and [Supplemental Data](#)). It is even possible that nonlinearities in the combination of eye and hand gain fields could explain the inaccuracies seen with reaching to targets in the far periphery (Bock, 1986; Enright, 1995; Henriques et al., 1998; Lewald and Ehrenstein, 2000; Medendorp and Crawford, 2002). Another interesting possibility is that these inaccuracies arise from the fact that the magnitude of the eye gain fields are slightly larger than arm gain fields; this possibility could be tested in a modeling study.

In three dimensions, the transformation between eye-centered and hand-centered target location is more complex than merely shifting the origin by the eye-hand distance (Soechting and Flanders, 1992; McIntyre et al., 1997; Blohm and Crawford, 2007; Blohm et al., 2009). Whether the representations in PRR can account for these higher-order issues is a matter for future study. It is also an open question whether and how PRR gain fields might account for eye-hand distances in depth.

In summary, the finding that eye and hand gain fields in individual PRR neurons are systematically related to one another provides strong physiological support for the hypothesis that gain fields are indeed used to perform specific computational tasks and strongly supports the idea that PRR is involved in encoding targets for visually-guided reaching.

EXPERIMENTAL PROCEDURES

Behavioral Tasks

We recorded neurons from two monkeys (*Macaca mulatta*) (see Supplemental Experimental Procedures for general recording procedures). In the preferred direction mapping task, animals made center-out arm movements while maintaining central fixation. Animals first fixated and pointed at a blue center target (2.4° × 2.4°, within 4° radius). A peripheral target (2.4° × 2.4°) appeared at one of 16 locations at 12°–14° eccentricity. Following a variable delay period (800–1200 ms), the center target shrank to a single pixel (0.3° × 0.3°) to signal the animal to make reaching movement to the target without breaking eye fixation. This task was used to determine the preferred direction, that is, the direction associated with the maximum neuronal response.

In the gain field task (Figure 1A), one initial “eye” target and one initial “hand” target were illuminated simultaneously (both 0.9° × 0.9°). Monkeys first fixated the initial eye target at one of three possible positions (P1–P3; spaced 7.5° apart), then touched the initial hand target (P1–P3). One possible target (either the initial eye or hand target) was always at the center of the screen, directly in front of the animal. The other two possible targets were located ± 7.5° along an imaginary line through the center of the screen and perpendicular to the cell’s preferred direction, as determined in the preferred direction mapping task. Five different configurations of the starting eye fixation (orbital eye position) and hand (pointed position) targets were used (see box in Figure 1A). Four hundred fifty ms after the animal touched and fixated the initial hand and eye target, a peripheral target (2.4° × 2.4°) for a final reach appeared at one of eight possible target locations. On each trial, animals maintained the initial eye and hand position (within 4° and 5° of the center, respectively) for a variable delay period (900–1300 ms) after the peripheral target onset. The initial eye and hand targets then shrank to a single pixel, cueing the animal to touch the peripheral target (within 5°–6°) without moving the eyes from the eye target. For the current study, we describe only the five targets in or near the preferred direction (T1–T5 in Figure 1A; spaced 7.5° apart), lying on a line perpendicular to the preferred direction and 12°–14° away from the center target (P2 to T3). There was also one target opposite to the preferred direction and two targets orthogonal to the preferred direction, all at 12°–14° eccentricity. These three additional targets lay well outside the response field of the cells, and were included only to make target position less predictable, expanding the range of target locations from ± 45 deg to a full 360°. For each cell we collected 8.0 ± 1.1 repetitions (mean and mode ± SD) of each trial type.

Data Analysis

We computed the mean spike rate in a 200 ms “visual” interval (50 to 250 ms from target onset time), in a 700 ms delay period (850 to 150 ms before the time of the go signal), and in a 250 ms perimovement period (200 ms before to 50 ms after movement onset). Similar results were obtained using slightly different time intervals and alignment points (e.g., a delay period from 150 to 850 ms after target onset). In order to examine the relationship between eye and hand gain fields after acquisition of the initial eye and hand targets but prior to the onset of a final reach target, we analyzed the activity from 400 ms before target onset (100 ms after acquiring the initial eye and hand targets) to 25 ms before target onset (“pretarget interval”).

We fitted mean spike rates from the visual, delay or movement intervals from individual cells in the 25 principal conditions (5 initial conditions × 5 targets) to a nonlinear seven parameter model:

$$Firing\ rate = pa \times \exp\left(\frac{-(\theta - mid)^2}{2 \times sd^2}\right) \times (1 + E \times gEye + H \times gHand) + k, \quad (1)$$

$$where\ \theta = \tan^{-1}\left(\frac{T - (weight \times E + (1 - weight) \times H)}{ecc}\right).$$

The model combines Gaussian tuning for a peripheral target with eye and hand gain fields. We refer to Equation 1 as “the full model” in the text. The fit was performed using the *nls* function in the R statistics package (www.R-project.org). The model inputs were the 25 mean firing rates (spikes/s), the eccentricity of the central target (*ecc*, the distance between P2 and T3 in Figure 1A), the target displacement away from the central target (*T*, the distance between the target and T3), and the displacement of the initial eye (*E*) and hand (*H*) targets from the center position (P2). All distances are degrees of visual angle. The parameters that were fit from these data were the baseline (*k*) and peak amplitudes of modulation (*pa*) (spikes/s); the offset of the Gaussian tuning curve from the central target (T3) (*mid*) and its standard deviation (*sd*), both in degrees of visual angle; the amplitudes of the eye position gain field (*gEye*) and the hand position gain field (*gHand*), both in fractional modulation per degree; and a unitless weight parameter (*weight*). The *weight* parameter determined the frame of reference for the Gaussian tuning, with weights of 1 or 0 corresponding to eye or hand-centered tuning, respectively. Note that both our eye- and hand-centered frames of reference are constrained to lie within the plane of the screen on which targets were presented and touches were performed. Because the screen was flat, the distance of the points from the eyes and body changed with eccentricity. We did not take this into account in our model.

During the fitting procedure, the parameters were constrained as follows: from –5 to 100 sp/s for *k*, from 0 to 300 sp/s for *pa*, –1.5 to 2.5 for *weight*, –0.15 to +0.15 (–15% to +15%) of modulation per degree for *gEye* and *gHand*, –45° to 45° for *mid*, and 15° to 60° for *sd*. These constraints were based on previously recorded data and by inspection of model fits. The fitting procedure was identical for all of the alternate models, described below and in the Results: the model with a single distance gain field term (Equation 2), the model with no gain field terms, and the multiplicative gain field model (Equation 3).

The details of the paradigm, including the number of targets, target spacing and eccentricity, was established using a series of simulations. We simulated neuronal responses to a wide variety of task designs, using idealized cells whose characteristics (tuning width, response variability, etc) were derived from PRR cells we had recorded in previous studies (Snyder et al., 1997; Calton et al., 2002; Chang et al., 2008). We varied the task parameters, used our idealized cells to generate artificial data, and then analyzed those data in order to optimize the task design and to ensure that the fitting procedure was reliable.

Details of Gain Field Modeling

If eye and hand position gain fields are negatively coupled, that is, if changes in eye position (*E*) result in a response modulation of “*E* × *g*,” and changes in hand position (*H*) result in a modulation of “*H* × (–*g*),” then the gain field portion of Equation 1 can be simplified:

$$E \times g + H \times (-g) = (E - H) \times g. \quad (2)$$

In words, the eye and hand position gain fields are replaced by a single gain field for the signed distance between the eyes and the hand.

Equation 2 assumes that eye and hand gain fields simply add together in a linear fashion. An alternate model embodies a multiplicative relationship between the eye and hand gain fields:

$$Firing\ rate = pa \times \exp\left(\frac{-(\theta - mid)^2}{2 \times sd^2}\right) \times (1 + E \times gEye) \times (1 + H \times gHand) + k, \quad (3)$$

$$where\ \theta = \tan^{-1}\left(\frac{T - (weight \times E + (1 - weight) \times H)}{ecc}\right).$$

In our task conditions, parameters *E* and *H* were never both nonzero. As a result, the fit of our data to this model is identical to the fit of the full model (Equation 1). More generally, however, the difference between the additive and multiplicative model is small under many circumstances:

$$\begin{aligned} \text{Additive} &: 1 + E \times g - H \times g \\ \text{Multiplicative} &: (1 + E \times g) \times (1 - H \times g) \\ &= 1 + E \times g - H \times g - E \times H \times g^2 \end{aligned} \quad (4)$$

The difference term, EHg^2 , is small when the eye or hand positions are close to central position, as was the case in our design (7.5°) and as is often (though not always) the case in normal behavior, since primates tend to aim their eyes and head toward the center of their workspace. If we had used starting eye and hand positions 50 deg apart then the additive and multiplicative models would have differed by 33% (based on the median value of the measured gain field strength, 2.3% per deg). However, in our paradigm, with the eye and hand within 15° of one another, the two models differ by less than 3%. Thus, in our task and in many natural behaviors, similar and opposite eye and hand gain fields can be approximated using a single gain field term based on the signed distance between the eyes and the hand (Equation 4).

Evaluation of Model Fits

A total of 259 neurons were recorded from PRR in two monkeys. Model fits were judged based on how well the model accounted for firing rate. We took both the strength of the Gaussian tuning and the overall variance explained by the model into account. We combined these two factors into a single measure by multiplying variance explained (r^2) by the peak modulation of the Gaussian fit (sp/s) to obtain “spike-variance explained” (sp/s). We accepted neurons with a criterion value of ≥ 5 sp/s of spike-variance explained. Acceptance criteria based on different criterion values of spike-variance explained (e.g., Figure 3B), on variance explained alone, or Chi-square tests of the goodness of fit, all resulted in similar conclusions regarding the relationship between eye and hand gain fields. Even when we considered all cells for which the model converged on a solution (255, or 98%), the hand and eye gain field parameters were inversely related.

Model Comparisons

A sequential F test was used to compare the quality of fits between the full model and a reduced model that lacked either an eye gain field (g_{Eye}), a hand gain field term (g_{Hand}), or both gain terms. Cells were classified as having a gain field if they showed a significant improvement in the full model compared to at least one of the two reduced models (without g_{Eye} or g_{Hand}) (F test, $p < 0.025$). The F ratio for each cell was obtained using

$$F = \frac{\frac{(RSS_{reduced} - RSS_{full})}{(N_{full} - N_{reduced})}}{\frac{RSS_{full}}{(DF_{full} - 1)}} \quad (5)$$

$RSS_{reduced}$ and RSS_{full} refer to the root mean square values for the reduced and the full model, respectively. Similarly, N_{full} and $N_{reduced}$ refer to the number of parameters for each model, and DF_{full} refers to the degrees of freedom of the full model.

In order to ask whether the ratio of eye to hand gain fields was really -1 or some other ratio (Figure 4B), we fit the data from all cells to a series of models similar to Equation 2 but with different fixed ratios between the eye and hand position gain field terms. Ratios of $-4.5:1$ to $+4.5:1$, at intervals of 0.2, were tested. Across each of the 45 models, cells for which the model did not converge were excluded (no more than 5% of all cells).

Neural Network Simulations

A three-layer feed-forward network was used for the simulation (Zipser and Andersen, 1988). The input layer consisted of 61 retinal inputs (mapped from -120° to $+120^\circ$), two eye position inputs and two hand position inputs. The retinal inputs were activated in accordance with a Gaussian input representing an eye-centered target location (peak locations ranged from -45° to 45° , $sd = 11^\circ$). The eye and hand position inputs were configured to be activated proportional to eye and hand position in the range from -20° to $+20^\circ$. The network was trained using a back-propagation algorithm to compute a tuning curve for the hand-centered location of a target according to the equation

$$H_C = E_C + (E_P - H_P), \quad (6)$$

where H_C , E_C , E_P , and H_P represent hand-centered target location, eye-centered target location, eye position, and hand position, respectively. There were 24 hidden units and 61 output units. Output units were mapped from -120° to $+120^\circ$.

SUPPLEMENTAL DATA

Supplemental Data include Supplemental Results, Supplemental Discussion, and five figures and can be found with this article online at [http://www.cell.com/neuron/supplemental/S0896-6273\(09\)00887-3](http://www.cell.com/neuron/supplemental/S0896-6273(09)00887-3).

ACKNOWLEDGMENTS

This work was supported by National Eye Institute and the National Institute of Mental Health. We thank J. Douglas Crawford for helpful discussions regarding reference frame transformations, Greg DeAngelis assistance in experimental design, Aaron Batista, Krishna Shenoy, and Chris Fetsch for comments on the manuscript, and Michael Goldberg for discussions on gain fields. We also thank Jason Vytalil and Justin Baker for MR imaging, and Tom Malone, Emelia Proctor, and Trevor Shew for technical assistance.

Accepted: October 18, 2009

Published: December 9, 2009

REFERENCES

- Andersen, R.A., and Mountcastle, V.B. (1983). The influence of the angle of gaze upon the excitability of the light-sensitive neurons of the posterior parietal cortex. *J. Neurosci.* **3**, 532–548.
- Andersen, R.A., Bracewell, R.M., Barash, S., Gnadt, J.W., and Fogassi, L. (1990). Eye position effects on visual, memory, and saccade-related activity in areas LIP and 7a of macaque. *J. Neurosci.* **10**, 1176–1196.
- Andersen, R.A., Snyder, L.H., Batista, A.P., Buneo, C.A., and Cohen, Y.E. (1998). Posterior parietal areas specialized for eye movements (LIP) and reach (PRR) using a common coordinate frame. *Novartis Found. Symp.* **218**, 109–122; discussion 122–128, 171–175.
- Avillac, M., Deneve, S., Olivier, E., Pouget, A., and Duhamel, J.R. (2005). Reference frames for representing visual and tactile locations in parietal cortex. *Nat. Neurosci.* **8**, 941–949.
- Batista, A.P. (1999). Contributions of parietal cortex to reach planning. (PhD dissertation, California Institute of Technology). 81–82.
- Batista, A.P., Buneo, C.A., Snyder, L.H., and Andersen, R.A. (1999). Reach plans in eye-centered coordinates. *Science* **285**, 257–260.
- Batista, A.P., Santhanam, G., Yu, B.M., Ryu, S.I., Afshar, A., and Shenoy, K.V. (2007). Reference frames for reach planning in macaque dorsal premotor cortex. *J. Neurophysiol.* **98**, 966–983.
- Battaglia-Mayer, A., Ferraina, S., Genovesio, A., Marconi, B., Squatrito, S., Molinari, M., Lacquaniti, F., and Caminiti, R. (2001). Eye-hand coordination during reaching. II. An analysis of the relationships between visuomanual signals in parietal cortex and parieto-frontal association projections. *Cereb. Cortex* **11**, 528–544.
- Blohm, G., and Crawford, J.D. (2007). Computations for geometrically accurate visually guided reaching in 3-D space. *J. Vis.* **7**, 4.1–4.22.
- Blohm, G., Keith, G.P., and Crawford, J.D. (2009). Decoding the cortical transformations for visually guided reaching in 3D space. *Cereb. Cortex* **19**, 1372–1393.
- Bock, O. (1986). Contribution of retinal versus extraretinal signals towards visual localization in goal-directed movements. *Exp. Brain Res.* **64**, 476–482.
- Boussaoud, D., Joffrais, C., and Bremmer, F. (1998). Eye position effects on the neuronal activity of dorsal premotor cortex in the macaque monkey. *J. Neurophysiol.* **80**, 1132–1150.
- Boynton, G.M. (2009). A framework for describing the effects of attention on visual responses. *Vision Res.* **49**, 1129–1143.
- Bradley, D.C., Maxwell, M., Andersen, R.A., Banks, M.S., and Shenoy, K.V. (1996). Mechanisms of heading perception in primate visual cortex. *Science* **273**, 1544–1547.
- Bremmer, F., Pouget, A., and Hoffmann, K.P. (1998). Eye position encoding in the macaque posterior parietal cortex. *Eur. J. Neurosci.* **10**, 153–160.

- Brochic, P.R., Andersen, R.A., Snyder, L.H., and Goodman, S.J. (1995). Head position signals used by parietal neurons to encode locations of visual stimuli. *Nature* 375, 232–235.
- Brozovic, M., Gail, A., and Andersen, R.A. (2007). Gain mechanisms for contextually guided visuomotor transformations. *J. Neurosci.* 27, 10588–10596.
- Bullock, D., and Grossberg, S. (1988). Neural dynamics of planned arm movements: emergent invariants and speed-accuracy properties during trajectory formation. *Psychol. Rev.* 95, 49–90.
- Buneo, C.A., Jarvis, M.R., Batista, A.P., and Andersen, R.A. (2002). Direct visuomotor transformations for reaching. *Nature* 416, 632–636.
- Burnod, Y., Grandguillaume, P., Otto, I., Ferraina, S., Johnson, P.B., and Caminiti, R. (1992). Visuomotor transformations underlying arm movements toward visual targets: a neural network model of cerebral cortical operations. *J. Neurosci.* 12, 1435–1453.
- Calton, J.L., Dickinson, A.R., and Snyder, L.H. (2002). Non-spatial, motor-specific activation in posterior parietal cortex. *Nat. Neurosci.* 5, 580–588.
- Caminiti, R., Johnson, P.B., Galli, C., Ferraina, S., and Burnod, Y. (1991). Making arm movements within different parts of space: the premotor and motor cortical representation of a coordinate system for reaching to visual targets. *J. Neurosci.* 11, 1182–1197.
- Caminiti, R., Ferraina, S., and Johnson, P.B. (1996). The sources of visual information to the primate frontal lobe: a novel role for the superior parietal lobule. *Cereb. Cortex* 6, 319–328.
- Chang, S.W., Dickinson, A.R., and Snyder, L.H. (2008). Limb-specific representation for reaching in the posterior parietal cortex. *J. Neurosci.* 28, 6128–6140.
- Cohen, Y.E., and Andersen, R.A. (2000). Reaches to sounds encoded in an eye-centered reference frame. *Neuron* 27, 647–652.
- Connor, C.E., Gallant, J.L., Preddie, D.C., and Van Essen, D.C. (1996). Responses in area V4 depend on the spatial relationship between stimulus and attention. *J. Neurophysiol.* 75, 1306–1308.
- Crawford, J.D., and Guitton, D. (1997). Visual-motor transformations required for accurate and kinematically correct saccades. *J. Neurophysiol.* 78, 1447–1467.
- Crawford, J.D., and Vilis, T. (1991). Axes of eye rotation and Listing's law during rotations of the head. *J. Neurophysiol.* 65, 407–423.
- Crawford, J.D., Cadera, W., and Vilis, T. (1991). Generation of torsional and vertical eye position signals by the interstitial nucleus of Cajal. *Science* 252, 1551–1553.
- Crawford, J.D., Henriques, D.Y., and Vilis, T. (2000). Curvature of visual space under vertical eye rotation: implications for spatial vision and visuomotor control. *J. Neurosci.* 20, 2360–2368.
- Crawford, J.D., Medendorp, W.P., and Marotta, J.J. (2004). Spatial transformations for eye-hand coordination. *J. Neurophysiol.* 92, 10–19.
- Desmurget, M., Epstein, C.M., Turner, R.S., Prablanc, C., Alexander, G.E., and Grafton, S.T. (1999). Role of the posterior parietal cortex in updating reaching movements to a visual target. *Nat. Neurosci.* 2, 563–567.
- Dickinson, A.R., Calton, J.L., and Snyder, L.H. (2003). Nonspatial saccade-specific activation in area LIP of monkey parietal cortex. *J. Neurophysiol.* 90, 2460–2464.
- Dobbins, A.C., Jee, R.M., Fiser, J., and Allman, J.M. (1998). Distance modulation of neural activity in the visual cortex. *Science* 281, 552–555.
- Enright, J.T. (1995). The non-visual impact of eye orientation on eye-hand coordination. *Vision Res.* 35, 1611–1618.
- Fattori, P., Gamberini, M., Kutz, D.F., and Galletti, C. (2001). 'Arm-reaching' neurons in the parietal area V6A of the macaque monkey. *Eur. J. Neurosci.* 13, 2309–2313.
- Galletti, C., and Battaglini, P.P. (1989). Gaze-dependent visual neurons in area V3A of monkey prestriate cortex. *J. Neurosci.* 9, 1112–1125.
- Galletti, C., Battaglini, P.P., and Fattori, P. (1995). Eye position influence on the parieto-occipital area PO (V6) of the macaque monkey. *Eur. J. Neurosci.* 7, 2486–2501.
- Galletti, C., Fattori, P., Kutz, D.F., and Battaglini, P.P. (1997). Arm movement-related neurons in the visual area V6A of the macaque superior parietal lobule. *Eur. J. Neurosci.* 9, 410–413.
- Galletti, C., Fattori, P., Kutz, D.F., and Gamberini, M. (1999). Brain location and visual topography of cortical area V6A in the macaque monkey. *Eur. J. Neurosci.* 11, 575–582.
- Goldberg, M.E., Bisley, J., Powell, K.D., Gottlieb, J., and Kusunoki, M. (2002). The role of the lateral intraparietal area of the monkey in the generation of saccades and visuospatial attention. *Ann. N Y Acad. Sci.* 956, 205–215.
- Gottlieb, J.P., Kusunoki, M., and Goldberg, M.E. (1998). The representation of visual salience in monkey parietal cortex. *Nature* 391, 481–484.
- Graziano, M.S. (1999). Where is my arm? The relative role of vision and proprioception in the neuronal representation of limb position. *Proc. Natl. Acad. Sci. USA* 96, 10418–10421.
- Graziano, M.S., Cooke, D.F., and Taylor, C.S. (2000). Coding the location of the arm by sight. *Science* 290, 1782–1786.
- Groh, J.M., and Sparks, D.L. (1996). Saccades to somatosensory targets. III. eye-position-dependent somatosensory activity in primate superior colliculus. *J. Neurophysiol.* 75, 439–453.
- Groh, J.M., Trause, A.S., Underhill, A.M., Clark, K.R., and Inati, S. (2001). Eye position influences auditory responses in primate inferior colliculus. *Neuron* 29, 509–518.
- Guthrie, B.L., Porter, J.D., and Sparks, D.L. (1983). Corollary discharge provides accurate eye position information to the oculomotor system. *Science* 221, 1193–1195.
- Henriques, D.Y., Klier, E.M., Smith, M.A., Lowy, D., and Crawford, J.D. (1998). Gaze-centered remapping of remembered visual space in an open-loop pointing task. *J. Neurosci.* 18, 1583–1594.
- Herter, T.M., Kurtzer, I., Cabel, D.W., Haunts, K.A., and Scott, S.H. (2007). Characterization of torque-related activity in primary motor cortex during a multijoint postural task. *J. Neurophysiol.* 97, 2887–2899.
- Kusunoki, M., Gottlieb, J., and Goldberg, M.E. (2000). The lateral intraparietal area as a salience map: the representation of abrupt onset, stimulus motion, and task relevance. *Vision Res.* 40, 1459–1468.
- Lacquaniti, F., and Caminiti, R. (1998). Visuo-motor transformations for arm reaching. *Eur. J. Neurosci.* 10, 195–203.
- Lal, R., and Friedlander, M.J. (1990). Effect of passive eye position changes on retinogeniculate transmission in the cat. *J. Neurophysiol.* 63, 502–522.
- Lewald, J., and Ehrenstein, W.H. (2000). Visual and proprioceptive shifts in perceived egocentric direction induced by eye-position. *Vision Res.* 40, 539–547.
- Lewis, J.W., and Van Essen, D.C. (2000a). Mapping of architectonic subdivisions in the macaque monkey, with emphasis on parieto-occipital cortex. *J. Comp. Neurol.* 428, 79–111.
- Lewis, J.W., and Van Essen, D.C. (2000b). Corticocortical connections of visual, sensorimotor, and multimodal processing areas in the parietal lobe of the macaque monkey. *J. Comp. Neurol.* 428, 112–137.
- Lewis, R.F., Gaymard, B.M., and Tamargo, R.J. (1998). Efference copy provides the eye position information required for visually guided reaching. *J. Neurophysiol.* 80, 1605–1608.
- Marzocchi, N., Breveglieri, R., Galletti, C., and Fattori, P. (2008). Reaching activity in parietal area V6A of macaque: eye influence on arm activity or retinocentric coding of reaching movements? *Eur. J. Neurosci.* 27, 775–789.
- Mays, L.E., and Sparks, D.L. (1980). Dissociation of visual and saccade-related responses in superior colliculus neurons. *J. Neurophysiol.* 43, 207–232.
- Mazzoni, P., Andersen, R.A., and Jordan, M.I. (1991). A more biologically plausible learning rule for neural networks. *Proc. Natl. Acad. Sci. USA* 88, 4433–4437.
- McIntyre, J., Stratta, F., and Lacquaniti, F. (1997). Viewer-centered frame of reference for pointing to memorized targets in three-dimensional space. *J. Neurophysiol.* 78, 1601–1618.

- Medendorp, W.P., and Crawford, J.D. (2002). Visuospatial updating of reaching targets in near and far space. *Neuroreport* 13, 633–636.
- Mullette-Gillman, O.A., Cohen, Y.E., and Groh, J.M. (2009). Motor-related signals in the intraparietal cortex encode locations in a hybrid, rather than eye-centered reference frame. *Cereb. Cortex* 19, 1761–1775.
- Nakamura, K., Chung, H.H., Graziano, M.S., and Gross, C.G. (1999). Dynamic representation of eye position in the parieto-occipital sulcus. *J. Neurophysiol.* 81, 2374–2385.
- Pare, M., and Guitton, D. (1998). Brain stem omnipause neurons and the control of combined eye-head gaze saccades in the alert cat. *J. Neurophysiol.* 79, 3060–3076.
- Pesaran, B., Nelson, M.J., and Andersen, R.A. (2006). Dorsal premotor neurons encode the relative position of the hand, eye, and goal during reach planning. *Neuron* 51, 125–134.
- Poggio, T. (1990). A theory of how the brain might work. *Cold Spring Harb. Symp. Quant. Biol.* 55, 899–910.
- Pouget, A., and Sejnowski, T.J. (1994). A neural model of the cortical representation of egocentric distance. *Cereb. Cortex* 4, 314–329.
- Pouget, A., and Snyder, L.H. (2000). Computational approaches to sensorimotor transformations. *Nat. Neurosci.* 3 (Suppl), 1192–1198.
- Pouget, A., Deneve, S., and Duhamel, J.R. (2002). A computational perspective on the neural basis of multisensory spatial representations. *Nat. Rev. Neurosci.* 3, 741–747.
- Prevosto, V., Graf, W., and Ugolini, G. (2009). Posterior parietal cortex areas MIP and LIPv receive eye position and velocity inputs via ascending preposito-thalamo-cortical pathways. *Eur. J. Neurosci.* 30, 1151–1161.
- Quiñero, R., Snyder, L.H., Batista, A.P., Cui, H., and Andersen, R.A. (2006). Movement intention is better predicted than attention in the posterior parietal cortex. *J. Neurosci.* 26, 3615–3620.
- Ren, L., Khan, A.Z., Blohm, G., Henriques, D.Y., Sergio, L.E., and Crawford, J.D. (2006). Proprioceptive guidance of saccades in eye-hand coordination. *J. Neurophysiol.* 96, 1464–1477.
- Robinson, D.L., McClurkin, J.W., and Kertzman, C. (1990). Orbital position and eye movement influences on visual responses in the pulvinar nuclei of the behaving macaque. *Exp. Brain Res.* 82, 235–246.
- Salinas, E., and Abbott, L.F. (1995). Transfer of coded information from sensory to motor networks. *J. Neurosci.* 15, 6461–6474.
- Salinas, E., and Abbott, L.F. (1996). A model of multiplicative neural responses in parietal cortex. *Proc. Natl. Acad. Sci. USA* 93, 11956–11961.
- Salinas, E., and Sejnowski, T.J. (2001). Gain modulation in the central nervous system: where behavior, neurophysiology, and computation meet. *Neuroscientist* 7, 430–440.
- Salinas, E., and Thier, P. (2000). Gain modulation: a major computational principle of the central nervous system. *Neuron* 27, 15–21.
- Scott, S.H., Sergio, L.E., and Kalaska, J.F. (1997). Reaching movements with similar hand paths but different arm orientations. II. Activity of individual cells in dorsal premotor cortex and parietal area 5. *J. Neurophysiol.* 78, 2413–2426.
- Shadmehr, R., and Wise, S.P. (2005). *The Computational Neurobiology of Reaching and Pointing: A Foundation for Motor Learning* (Cambridge, MA: MIT Press).
- Siegel, R.M., Raffi, M., Phinney, R.E., Turner, J.A., and Jando, G. (2003). Functional architecture of eye position gain fields in visual association cortex of behaving monkey. *J. Neurophysiol.* 90, 1279–1294.
- Smith, M.A., and Crawford, J.D. (2005). Distributed population mechanism for the 3-D oculomotor reference frame transformation. *J. Neurophysiol.* 93, 1742–1761.
- Snyder, L.H., Batista, A.P., and Andersen, R.A. (1997). Coding of intention in the posterior parietal cortex. *Nature* 386, 167–170.
- Snyder, L.H., Grieve, K.L., Brotchie, P., and Andersen, R.A. (1998). Separate body- and world-referenced representations of visual space in parietal cortex. *Nature* 394, 887–891.
- Snyder, L.H., Dickinson, A.R., and Calton, J.L. (2006). Preparatory delay activity in the monkey parietal reach region predicts reach reaction times. *J. Neurosci.* 26, 10091–10099.
- Sober, S.J., and Sabes, P.N. (2003). Multisensory integration during motor planning. *J. Neurosci.* 23, 6982–6992.
- Sober, S.J., and Sabes, P.N. (2005). Flexible strategies for sensory integration during motor planning. *Nat. Neurosci.* 8, 490–497.
- Soechting, J.F., and Flanders, M. (1992). Moving in three-dimensional space: frames of reference, vectors, and coordinate systems. *Annu. Rev. Neurosci.* 15, 167–191.
- Tweed, D., and Vilis, T. (1987). Implications of rotational kinematics for the oculomotor system in three dimensions. *J. Neurophysiol.* 58, 832–849.
- Van Opstal, A.J., Hepp, K., Suzuki, Y., and Henn, V. (1995). Influence of eye position on activity in monkey superior colliculus. *J. Neurophysiol.* 74, 1593–1610.
- Wang, X., Zhang, M., Cohen, I.S., and Goldberg, M.E. (2007). The proprioceptive representation of eye position in monkey primary somatosensory cortex. *Nat. Neurosci.* 10, 640–646.
- Weyand, T.G., and Malpeli, J.G. (1993). Responses of neurons in primary visual cortex are modulated by eye position. *J. Neurophysiol.* 69, 2258–2260.
- White, R.L., 3rd, and Snyder, L.H. (2004). A neural network model of flexible spatial updating. *J. Neurophysiol.* 91, 1608–1619.
- Xing, J., and Andersen, R.A. (2000). Models of the posterior parietal cortex which perform multimodal integration and represent space in several coordinate frames. *J. Cogn. Neurosci.* 12, 601–614.
- Zipser, D., and Andersen, R.A. (1988). A back-propagation programmed network that simulates response properties of a subset of posterior parietal neurons. *Nature* 331, 679–684.

Supplemental Data

Using a Compound Gain Field

to Compute a Reach Plan

Steve W.C. Chang, Charalampos Papadimitriou, and Lawrence H. Snyder

Supplemental Results and Discussion

The Degree of Correlation Between Eye and Hand Gain Fields

The slopes of the regressions in Figure 3 are close to but significantly smaller than -1 (all $p < 0.05$, linear regression). The gain field measurements might show deviations from having a slope of negative one because the gain fields are truly not perfectly correlated, because the measurement is contaminated by noise, or because of a combination of these two effects. Our regressions were type II (that is, the regression model assumed that there was uncertainty in the measurements of the values on both the x and y axes), and so noise would decrease the correlation but not systematically change the slope. Therefore the fact that the slopes were significantly different from minus one indicates that eye gain field strengths were stronger than hand gain field strengths at the population level. This may be because there are two separate populations of cells, one with matched gain fields and one with eye gain fields greater than hand (or perhaps even entirely lacking in hand gain fields). Alternatively, all cells may have slightly larger eye than hand gain fields. Our data do not allow us to make this distinction (but see legend of Supplemental Figure 5). To test whether measurement noise might also contribute to the fact that regression slopes were different from negative one, we plotted the distance of each point from the negative unity line as a function of spike-variance explained (Supplemental

Figure 5). Indeed, cells with high spike-variance explained all lay close to the negative unity line, while cells far from the line had low spike-variance explained. The 10% of cells with the highest spike-variance explained fell within the bottom 35% of deviations from the negative unity line, while the 10% of cells with the largest deviations from the negative unity line fell within the bottom 46% of spike-variance explained. Therefore we believe that measurement noise also plays a role in lowering the correlation between eye and hand position gain fields.

Linear Versus Multiplicative Combination of Eye and Hand Gain Fields

If gain fields combine multiplicatively instead of linearly (Equation 3 versus Equation 1, Experimental Procedures), then negatively correlated eye and hand gain fields would not form a single gain field encoding the signed distance between the fixation point and the hand (see Equation 4). If the point of gaze is far from the hand, then the effects are moderate, e.g., a 33% difference in predicted activity between an additive and a multiplicative model for an eye-hand distance of 50° of visual angle (based on the median 2.30%/deg distance gain field found in the present study). However, for the eye-hand distances used in the current study (7.5° and 15°), the difference between the additive and multiplicative models would be only 1% or 3%, respectively. Such a small effect would be buried in the measurement noise. Future experiments could help refine the model by using much larger separations between initial eye and hand position, establishing whether the interaction between eye and hand position gain fields is strictly linear (and therefore forms a perfect eye-hand distance gain field) or involves a non-linearity such as a multiplicative term (and therefore diverges from an eye-hand distance gain field for large peripheral eye or hand positions).

Further Characterization of Eye and Hand Gain Fields

Ideally, we would use more than three initial eye and hand positions in order to more precisely determine the shape of eye and hand position gain fields, and we would test for gain field interactions in all three dimensions. We suspect that, as in LIP, the gain fields of many but not all PRR neurons would be well fit by a linear function (e.g., Andersen and Mountcastle, 1983; Brotchie et al., 1995), and that gain fields will be present in multiple dimensions (Andersen et al., 1990), including the depth dimension. It would be particularly interesting to know whether the finding of equal magnitude but opposite directions of eye and hand gain fields applies across all three dimensions, and whether the *shape* of eye and hand gain fields are also matched. Because of the complexities of separating gain field effects from tuning curve shifts in multiple dimensions, these experiments will likely require chronically implanted electrode arrays from which very large data sets can be collected (Batista et al., 2007).

Supplemental Experimental Procedures

General Recording Procedures

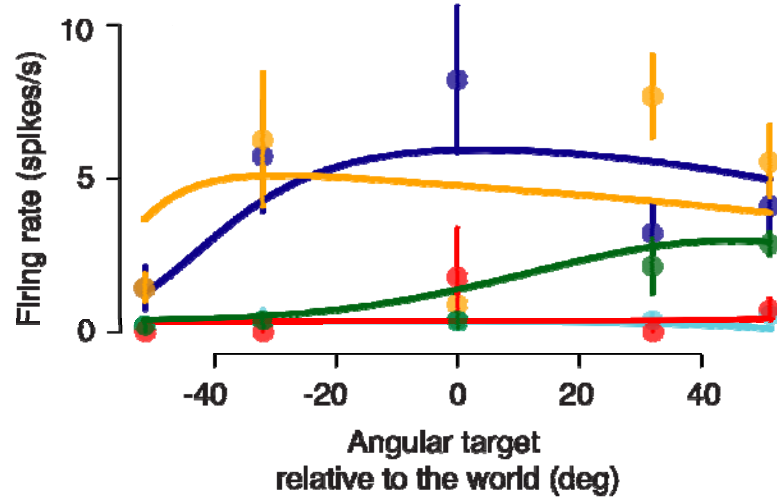
Eye position was monitored by the scleral search coil technique (CNC Engineering, Seattle, Washington). Hand position was monitored by a 13.2 x 13.2 cm custom-built touch panel that uses finely spaced (3 mm) horizontal and vertical infrared beams, 1-3 mm above a smooth surface (temporal resolution = 2 ms). A registered touch or release was defined as an incidence when a finger or fingers (typically an index finger or index and middle fingers together) broke the beams at a particular location(s) on the touch panel. The animals sat in a custom-designed monkey chair (Crist Instrument, Hagerstown, Maryland) with a fully open front

to provide unimpaired reaching movements. Visual stimuli were back-projected by a CRT projector onto the touch surface, which was mounted vertically, 25 cm in front of the animal. The recording room was sound-attenuating and light-proof, such that a dark-adapted human could detect no light when the projector was turned on but projecting no targets.

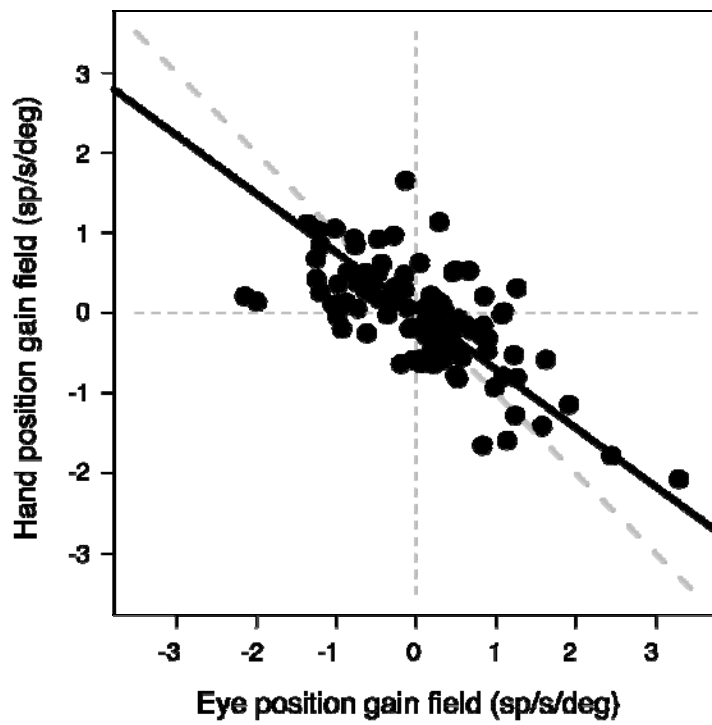
The touch screen was mounted such that the center was approximately aligned the line of sight when the eyes were estimated to be in primary position. The screen center then formed the origin of our coordinate system for measuring eye and hand position. All measurements are therefore in screen coordinates, i.e., the location at which gaze intercepts the screen, and the location at which the animal touches the screen. As a shorthand, we refer to these measurements throughout the text as eye and hand position, respectively.

We recorded neurons from two monkeys (*Macaca mulatta*). Extracellular recordings were made using glass-coated tungsten electrodes (Alpha Omega, Alpharetta, Georgia). Cells were recorded from the right hemisphere from monkey G and left hemisphere from monkey S, with each animal using its contralateral limb. For each signal we encountered, we used the mapping task to ascertain isolation, stability and the approximate preferred direction of that cell. For each stable, well-isolated single neuron that showed clear spatial tuning in the mapping task ($n = 259$), we ascertained the preferred direction from the mapping task and then ran the gain field task (below). These 259 cells represented about 60% of the ~450 signals we encountered. About 30% of the signals were rejected because of poor isolation or stability, and the remaining 10% were rejected because spatial tuning was absent or unclear. In this report we analyze the data of every one of the 259 cells in which we decided to run the gain field task. Because the decision to run or not run this task in a given cell was based solely on the results of the mapping task, the only bias in cell selection was in favor of cells with spatial tuning.

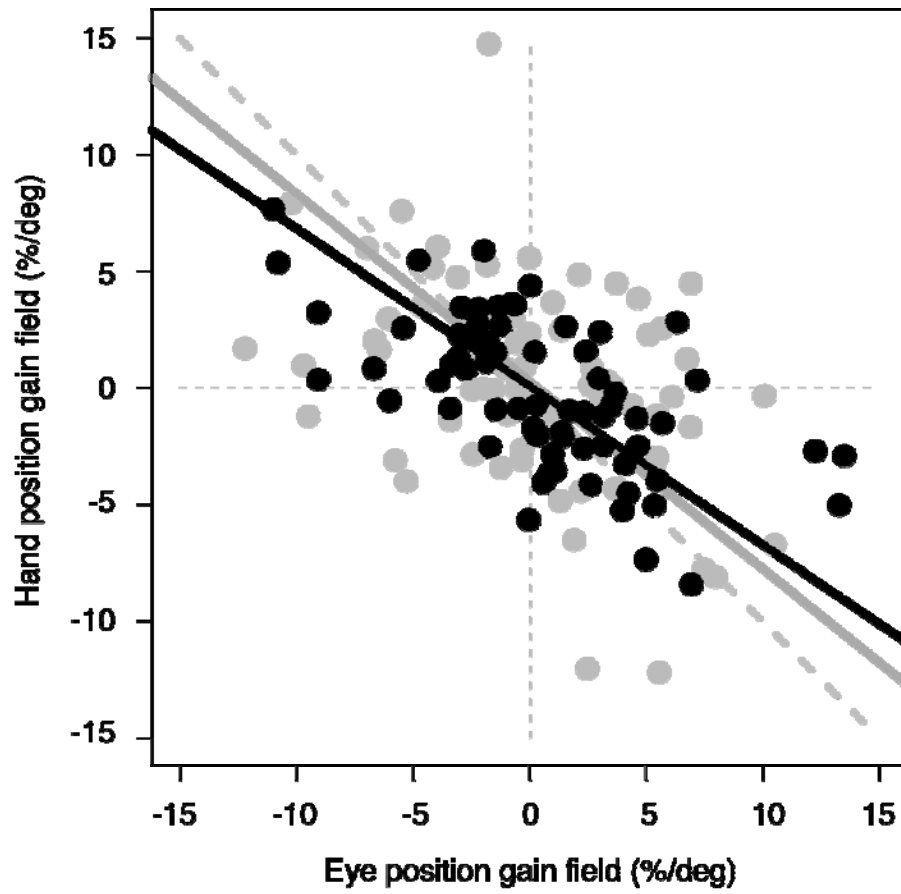
In order to guide the placement of our recording tracks and localize recording sites, we acquired high-resolution magnetic resonance images (MRI) of monkeys' brains with an MR lucent "phantom" in the recording chamber, using methods described elsewhere (Calton et al., 2002; Chang et al., 2008; Kalwani et al., 2009). Localization was accurate to within 1 mm, as determined by injecting and then visualizing MR-lucent manganese in the brain in several sessions. PRR cells straddle the boundary between MIP and V6A. A more precise anatomical label in terms of cortical areas or cortical topography is problematic. The boundaries of cortical areas in and around IPS are highly variable (Lewis and Van Essen, 2000a; Lewis and Van Essen, 2000b), and as can be seen from Figure 1C, the IPS and POS sulci are not discrete, but merge into one another. Thus the term parietal reach region emphasizes that this region is functional defined, not anatomically defined (Snyder et al., 1997; Buneo et al., 2002; Chang et al., 2008).



Supplemental Figure 1, Chang.Supp1.pdf

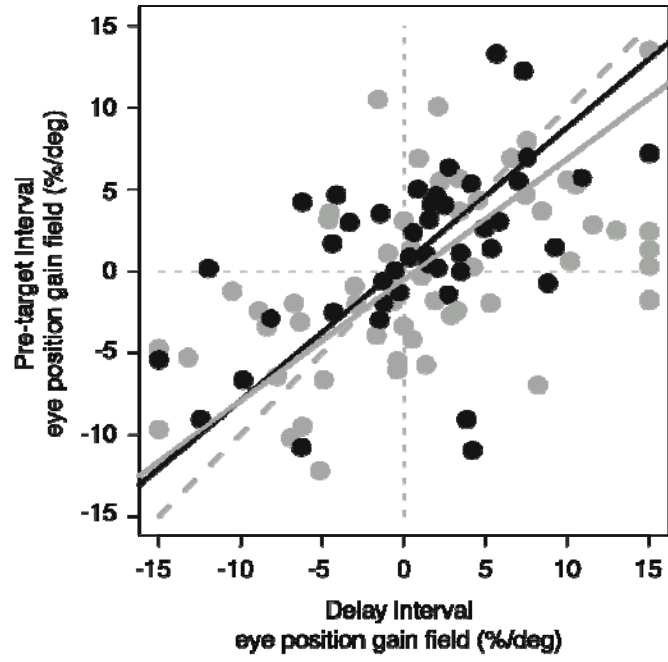


Supplemental Figure 2, Chang.Supp2.pdf

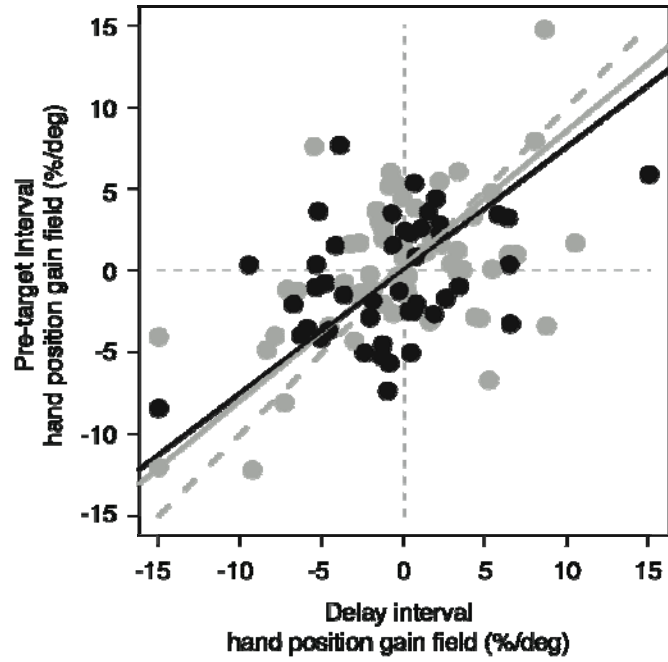


Supplemental Figure 3, Chang.Supp3.pdf

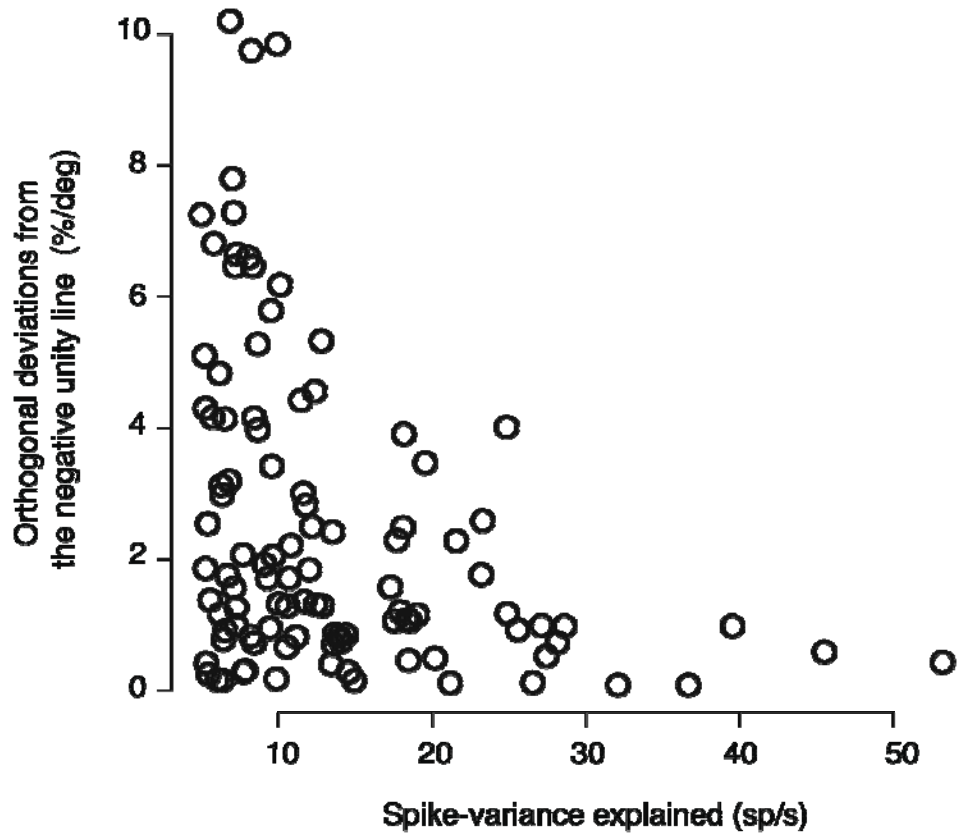
A



B



Supplemental Figure 4, Chang.Supp4.pdf



Supplemental Figure Legends

Supplemental Figure 1. A Neuron with High Variance Explained, but Low Spike-Variance Explained.

The full model explains 66% of the variance in firing rate, passing our 50% criterion. However, the modelled Gaussian modulation is only 2.6 sp/s, so that spike-variance is only 1.7 sp/s, failing both our 5 and 2 sp/s spike-variance explained criteria. Interestingly, the eye and gain fields were still similar in strength but opposite in sign (*Eyes Left* [cyan]: peak 0.54 0.26 sp/s, *Eyes Right* [dark blue]: 8.21 2.38 sp/s, *Hand Left* [yellow-orange]: 7.68 1.35 sp/s, *Hand Right* [red]: 1.79 1.59 sp/s; eye gain field: 0.39 sp/s per deg, hand gain field: -0.28 sp/s per deg). Format as in Fig. 2B.

Supplemental Figure 2. Negatively Coupled Eye and Hand Position Gain Fields Plotted Using Absolute Firing Rates.

The same data as in Figure 3A but without normalization (spikes/s/deg instead of %/deg). The solid black line represents the type II regression. We normalized by dividing absolute eye and hand gain fields by the same value (delay period firing rate for a reach in the preferred direction starting from the aligned condition). This normalization has minimal effect on the population statistics. The normalized gain field data have a correlation coefficient of -0.61 ($p < 0.00001$, Spearman's rank correlation) and a type II regression slope of -0.74, while the unnormalized (absolute) data have a correlation coefficient of -0.67 ($p < 0.00001$) and a type II regression slope of -0.73.

Supplemental Figure 3. The Distance Gain Field does not Require a Target.

The negative correlation between eye and hand position gain fields is present prior to the onset of a final reach target but after the acquisition of the initial eye and hand targets. Cells with at least 2 sp/s spike-variance explained are shown in grey; cells with at least 5 sp/s spike-variance explained are shown in black. Format otherwise similar to Figure 3A.

Supplemental Figure 4. Eye and Hand Gain Fields are Correlated Before and After the Onset of a Reach Target.

(A) The positive correlation between eye position gain fields before the onset of a reach target (pre-target interval) and after the onset of a reach target (delay interval). Cells with at least 2 sp/s spike-variance explained are shown in grey (Spearman's rank correlation, $r = 0.52$, $p < 0.00001$, $n = 104$), and cells with at least 5 sp/s spike-variance explained are shown in black ($r = 0.50$, $p < 0.001$, $n = 45$) (data points and type II regression slopes are shown). Format otherwise similar to Figure 3A.

(B) The positive correlation between hand position gain fields before the onset of a reach target (pre-target interval) and after the onset of a reach target (delay interval). Cells with at least 2 sp/s spike-variance explained are shown in grey ($r = 0.38$, $p < 0.0001$, $n = 104$), and cells with at least 5 sp/s spike-variance explained are shown in black ($r = 0.38$, $p < 0.05$, $n = 45$). Same format as in (A).

Supplemental Figure 5. The Evidence for a Distance Gain Field is Stronger for Cells Whose Activity is Well Explained by the Model.

A scatter plot of the orthogonal deviation from the negative unity line (%/deg) from Figure 3A (eye versus hand gain fields) plotted as a function of the spike-variance explained by the full model. Neurons that are well fit by the model (on the right side of the plot) are close to the negative unity line and therefore have amplitude-matched gain field strengths. Neurons that lie far from the line and therefore have eye and hand gain fields that are not matched are poorly fit by the model. Since the model allows eye and hand gain fields to vary independently, the poor fit of cells that lie far from the unity line suggests that there is not a separate, well-behaved population of eye-only gain field cells, but rather either that the data obtained from these cells that appear to be eye-only gain field cells was substantially degraded by noise, or else that the data from these cells would be better fit by a different model than the one we used.

Supplemental References

Andersen, R. A., Bracewell, R. M., Barash, S., Gnadt, J. W., and Fogassi, L. (1990). Eye position effects on visual, memory, and saccade-related activity in areas LIP and 7a of macaque. *J Neurosci* 10, 1176-1196.

Andersen, R. A., and Mountcastle, V. B. (1983). The influence of the angle of gaze upon the excitability of the light-sensitive neurons of the posterior parietal cortex. *J Neurosci* 3, 532-548.

Batista, A. P., Santhanam, G., Yu, B. M., Ryu, S. I., Afshar, A., and Shenoy, K. V. (2007). Reference frames for reach planning in macaque dorsal premotor cortex. *J Neurophysiol* 98, 966-983.

Brotchie, P. R., Andersen, R. A., Snyder, L. H., and Goodman, S. J. (1995). Head position signals used by parietal neurons to encode locations of visual stimuli. *Nature* 375, 232-235.

Buneo, C. A., Jarvis, M. R., Batista, A. P., and Andersen, R. A. (2002). Direct visuomotor transformations for reaching. *Nature* 416, 632-636.

Calton, J. L., Dickinson, A. R., and Snyder, L. H. (2002). Non-spatial, motor-specific activation in posterior parietal cortex. *Nat Neurosci* 5, 580-588.

Chang, S. W., Dickinson, A. R., and Snyder, L. H. (2008). Limb-specific representation for reaching in the posterior parietal cortex. *J Neurosci* 28, 6128-6140.

Kalwani, R. M., Bloy, L., Elliott, M. A., and Gold, J. I. (2009). A method for localizing microelectrode trajectories in the macaque brain using MRI. *J Neurosci Methods* 176, 104-111.

Lewis, J. W., and Van Essen, D. C. (2000a). Mapping of architectonic subdivisions in the macaque monkey, with emphasis on parieto-occipital cortex. *J Comp Neurol* 428, 79-111.

Lewis, J. W., and Van Essen, D. C. (2000b). Corticocortical connections of visual, sensorimotor, and multimodal processing areas in the parietal lobe of the macaque monkey. *J Comp Neurol* 428, 112-137.

Snyder, L. H., Batista, A. P., and Andersen, R. A. (1997). Coding of intention in the posterior parietal cortex. *Nature* 386, 167-170.